In-Situ CIR-FTIR Study of the Diffusion of Supercritical Hydrocarbons in Zeolite L

Murat G. Süer, Zissis Dardas, Yaping Lu, William R. Moser, and Yi H. Ma
Dept. of Chemical Engineering, Worcester Polytechnic Institute, Worcester, MA 01609

Cylindrical internal reflectance infrared spectroscopy (CIR-FTIR) was used for the determination of the transport properties of hydrocarbons in zeolite L at high temperatures and pressures. This was the first time that the intracrystalline diffusivity of hydrocarbons in microporous media could be determined under supercritical conditions by using a dynamic technique. The study investigated the self-diffusion of n-heptane, the counterdiffusion of n-hexane and 1-hexene, and the codiffusion of n-heptane and p-xylene in zeolite L under subcritical and supercritical conditions. The diffusion time constants obtained for the single and binary systems showed that the diffusion within the pore was reduced significantly under supercritical conditions (i.e., liquidlike behavior) as the hydrocarbon density within the pore was increased.

Introduction

The transport of organic and inorganic compounds in zeolites is a particularly interesting and complex phenomenon in terms of fundamental physical chemistry and in applications of zeolites, for example, separation processes or catalysis. Therefore, research in this area has grown tremendously in the past three decades to understand physicochemical behavior of liquids and gases in zeolites.

The activity and/or selectivity of zeolite catalysts in hydrocarbon catalysis depends on both the intrinsic activity of the active sites of the zeolite and the diffusion of reactants and products within the pores of the zeolite. Therefore, a good mechanistic understanding of these processes and development of new chemical processes are strongly dependent on the evaluation of the catalytic and transport properties of reactants and products at autogeneous reaction conditions.

For a long period of time, the key parameters of zeolitic diffusion (i.e., diffusion coefficients and activation energies of diffusion) were exclusively derived from static sorption and desorption kinetic measurements. Here, the preferred tool used was the microbalance that measured the gain or loss of weight with time due to the uptake or desorption of sorbate molecules (Riekert, 1970, 1971; Barrer, 1978; Ruthven, 1984). Other physical properties used rather than the weight change were the change of either volume or pressure, with one of them being constant. In the late 1960s and early 1970s an essentially different technique was introduced to study the diffusion of molecules in zeolites by means of nuclear magnetic resonance (NMR) spectroscopy (Resing, 1968; Karger and Caro, 1977). From these studies, it was shown that self-diffusion coefficients under equilibrium conditions could be evaluated from measurements of relaxation time. NMR spectroscopic studies for the determination of transport properties in zeolites were particularly successful with the application of "pulsed field gradient" (Karger et al., 1980; Karger and Pfeifer, 1987) and "fast tracer desorption" (Karger, 1982) techniques.

Besides the static methods, the use of dynamic techniques for the evaluation of transport properties of gases and liquids in porous media was quite successful (e.g., Ma et al., 1988; Lin and Ma, 1989a). The authors have used a chromatographic technique (i.e., high pressure liquid chromatography) to study diffusion properties both for gases and liquids in single and bidispersed porous catalysts. They concluded that nonlinear adsorption isotherms and intraparticle diffusivities in porous adsorbents can be determined simultaneously from the impulse chromatographic response peaks at different carrier flow rates and injection sample concentrations. The isotherms measured by the chromatographic technique were found to be in good agreement with the isotherms obtained by the static (batch) methods. These authors also reported a complete mathematical model for the evaluation of diffusion and adsorption coefficients in porous adsorbents (Lin and Ma,

Correspondence concerning this article should be addressed to Y. H. Ma.

1989b, 1990). The experimental results obtained for a variety of systems (i.e., alcohols in silicalite, polar and nonpolar liquids in aluminas) were also found to be in good agreement with the proposed mathematical model, proving the potential of the technique.

Eic and Ruthven (1988) introduced the "zero-length column method" that used a highly sensitive flame ionization detector (FID) to monitor the desorption of sorbate molecules previously equilibrated with the sorbate under controlled conditions. The technique was limited to only hydrocarbon sorbates because of the detector, and was proven especially useful for the study of strongly adsorbed species such as aromatic and polyaromatic hydrocarbons.

The dynamic chromatographic studies were followed by the development of dynamic spectroscopic methods for studying diffusion in zeolites. Karge and Niessen (1991) developed a novel infrared method that monitored the change (i.e., uptake or desorption) in the integrated intensity of an infrared band typical of the sorbate molecule by a fast-scanning FT-IR spectrometer. With this technique they have studied the self-diffusion (Karge and Niessen, 1991), counter- (Karge and Niessen, 1991; Niessen and Karge, 1993), and codiffusion (Niessen and Karge, 1993) of aromatic hydrocarbons (i.e., benzene, ethylbenzene, *p*-xylene) in pentasil zeolites. The only limitations of the IR technique for the study of the counter- and codiffusion of hydrocarbons in zeolites was that the IR bands of the two components should be well separated in the spectra.

The behavior of supercritical fluids (SCF's) has attracted a great deal of interest in recent years, and research in this area has led to a number of practical applications that are reviewed elsewhere (e.g., Kiran and Brennecke, 1993; Savage et al., 1995). In heterogeneous catalysis, the supercritical reaction media have been employed to regenerate porous catalysts by the *in situ* extraction of coke compounds (e.g., Tiltscher et al., 1981, 1984; Tiltscher and Hoffman, 1987; Saim and Subramaniam, 1990, 1991; Manos and Hoffman, 1991; Yokota and Fujimoto, 1991; Baptist-Nguyen and Subramaniam, 1992; Subramaniam and McCoy, 1994; Ginosar and Subramaniam, 1995; Lang et al., 1995). The cited advantages of supercritical processing over conventional gas-phase processing included enhanced activity maintenance, higher reaction rates, and desirable product selectivity. The main reason for such improvements was a result of the enhancements of the physicochemical properties of the fluid (Squires et al., 1983; Tiltscher and Hoffman, 1987) in the critical state (i.e., liquid-like density, hence high solvation power) that could result in the *in situ* extraction of low volatile components deactivating the catalyst (i.e., coke), together with the faster diffusion of the reaction products in the porous network (gaslike diffusivities).

The enhanced activities and desired product selectivities during hydrocarbon conversion processes under supercritical conditions are directly related to the interactions of reactants and products with the active sites of the catalysts, which may be influenced by the sorption and diffusion properties of these molecules within the micropores. However, the analysis of transport behavior of supercritical hydrocarbons in zeolites is experimentally difficult because of the severe operating conditions (high temperatures and pressures).

Previous transport studies for supercritical fluids are mainly concerned with the evaluation of binary diffusion coefficients. These coefficients are used in the correlation and prediction of mass-transfer coefficients for the design of separation processes. The publications in this area can be summarized as follows: Dahmen et al. (1990) measured the diffusion coefficients of organic compounds such as 2-propanone and 3-pentanone, in supercritical carbon dioxide; Jacob Sun and Chen (1985) studied the tracer diffusion of aromatic hydrocarbons such as benzene and toluene, in supercritical *n*-hexane. Both of these studies concluded that the diffusion coefficients in supercritical solvents are higher than in liquids, suggesting faster mass-transfer rates in the supercritical regime.

The only early work related to the current study was Lai and Tan (1993), who obtained effective diffusivities of toluene in activated carbon (AC) in the presence of supercritical carbon dioxide by using a sorption-rate technique in a spinning-basket reactor. The temperatures that they investigated were 35, 45, 55°C at pressures up to 163 bar (toluene is liquid at these conditions). The authors concluded that the effective diffusivities obtained at supercritical conditions were observed to be strongly dependent on CO_2 density, but weakly dependent on temperature and the amount of toluene adsorbed. The effective diffusivities generally decreased with increasing density at constant temperatures.

In view of the very limited data on intracrystalline diffusion coefficients of hydrocarbons at supercritical conditions inside porous catalysts, the objective of this study was to understand the effects of supercritical media on the transport behavior of hydrocarbons within porous catalysts by using a dynamic infrared technique (CIR-FTIR), which was developed earlier in our laboratories for the *in-situ* analysis of homogeneous catalytic reactions (Moser et al., 1985; Moser, 1992), as well as monitoring the progress (i.e., active site concentrations) of hydrocarbon conversion processes (i.e., catalytic cracking) at high temperatures and pressures (Dardas et al., 1996a). Using this technique, detailed mechanisms of hydrocarbon catalytic cracking and catalyst stabilization toward rapid deactivation under supercritical fluid conditions were elucidated for the first time (Süer et al., 1996a,b; Dardas et al., 1996b).

Experimental Studies

Catalyst and chemicals

The zeolite employed to study the intracrystalline diffusion of hydrocarbons was zeolite L supplied by UOP. The reason for using this zeolite was due to its unique wide channels (Barrer and Villiger, 1969), and unique catalytic properties in hydrocarbon aromatization processes (Derouane and Vanderveken, 1988). Preliminary experiments by examination of the Bronsted AlOH acidic sites and the color of the catalyst indicated that this catalyst showed almost no coke formation with a low degree of catalytic conversion ($\approx 1\%$) under the supercritical conditions of the hydrocarbons studied. This was of particular importance since coke formation will affect the transport properties within the pores (i.e., oligomerization of reactant hydrocarbons on active sites). The zeolite was in the H-L form, with no extra framework of Al and with a silica to alumina ratio of around 7. It had a surface area 420 m^2/g and pore volume 0.18 cc/g, with a particle-size distribution ranging from 0.2 to 1.2 μm (average 0.6 μm).

This study investigated (1) the self-diffusion of *n*-heptane, (2) the counter diffusion of *n*-hexane and 1-hexene, and (3) the codiffusion of *n*-heptane and *p*-xylene in zeolite L under subcritical and supercritical conditions. The hydrocarbons were purchased from Aldrich with 99+% purity. The experiments were conducted using a ZnSe crystal (reflecting element) that was purchased from Spectral Systems.

Methods and procedures

The experimental procedure and instrumentation required for the *in-situ* infrared analysis of a heterogeneous system at high temperatures and pressures by CIR-FTIR spectroscopy has been previously described in detail (Dardas et al., 1996a). The diffusion experiments were carried out in a specially designed cylindrical internal reflection (CIR) microreactor, mounted directly on the optical bench of a midrange FT-IR spectrometer (Nicolet 510P). The feed hydrocarbons were introduced using a precision metering, high-pressure, low-volume liquid pump. The experimental setup was built from 0.16-cm stainless-steel high-pressure lines, and included a downstream back-pressure regulator to adjust the system pressure, mass flowmeters, and pressure gauges. The flow system was designed to operate at temperatures up to 500°C and pressures up to 68 bar.

A ZnSe crystal of 0.64 cm in diameter and 8.26 cm long with conical ends polished at 45° to the axis was embedded in the reactor, and the catalyst was packed tightly in the annular space. The details of the reactor, crystal element, and basic principles involved in the CIR-IR technique were previously described (Dardas et al., 1996a).

A midrange infrared spectrometer (Nicolet 510P), continuously purged with nitrogen and equipped with a Mercury Cadmium Telluride-B detector was used to acquire all IR spectra. Unless otherwise specified, the IR spectra were collected at a spectral resolution of 4 cm^{-1} by coadding six scans to obtain the desired signal-to-noise ratio. This gave an acquisition time of 9 s for each spectrum. The changes in the integrated absorbance of the IR band typical of the sorbate molecule were monitored as a function of time until equilibrium (constant integrated intensity of the sorbate) was achieved. The supplied Nicolet software was used for spectral manipulation (ratioed to background, base line and spectral subtraction, and smoothing) and integration.

Evaluation of diffusion coefficients

The data of sorption kinetics obtained from the change in absorbance of typical hydrocarbon sorbates were evaluated through a solution of Fick's second law (Eq. 1) provided by Crank (1956) for diffusion into spheres with variable surface concentration:

$$\frac{\partial C}{\partial t} = D\left[\frac{\partial^2 C}{\partial r^2} + \frac{2}{r}\frac{\partial C}{\partial r}\right], \tag{1}$$

with the initial and boundary conditions;

$$C = Co \qquad r = 0 \quad t = 0 \tag{2}$$

$$dC/dr = 0 \qquad r = 0 \quad t > 0 \tag{3}$$

$$C = a\phi(t) \qquad r = a \quad t > 0. \tag{4}$$

The solution of Eq. 1 with the initial and boundary conditions given in Eqs. 2 to 4 is

$$C = -\frac{2D}{\pi a}\sum_{n=1}^{\infty}(-1)^n \exp\left(-\frac{D\pi^2 n^2}{a^2}\right) n\pi \sin \times\left(\frac{n\pi r}{a}\right)\int_0^t \exp\left(-\frac{Dn^2\pi^2}{a^2}t\right)\phi(t)\,dt, \tag{5}$$

where C, D, t, r, and a denote the concentration, diffusion coefficient, time, radial coordinate, and radius of the crystallite, respectively. The time lag occurs because of the partial pressure of the sorbate under study is not instantaneously established at the location of the sample due to the finite flow rate. The time lag is best described by Eq. 6:

$$\phi(t) = C_o[1 - \exp(-\beta t)], \tag{6}$$

where C_0 and β stand for the surface concentration and a time constant, respectively. With a constant diffusion coefficient, D (not dependent on concentration), the normalized sorption curve is given by the following equation:

$$\frac{M_t}{M_\infty} = 1 - \left(\frac{3D}{\beta a^2}\right)\exp\left(-\beta t\left(1 - \left(\frac{\beta a^2}{D}\right)^{1/2}\cot\left(\frac{\beta a^2}{D}\right)^{1/2}\right)\right) + \frac{6\beta a^2}{\pi^2 D}\sum_{n=1}^{\infty}\frac{\exp(-Dn^2\pi^2 t/a^2)}{n^2\left(n^2\pi^2 - \frac{\beta a^2}{D}\right)}, \tag{7}$$

where M_t ($\sim A_t$, i.e., absorbance) is the amount of sorbate taken up at time t, whereas M_α ($\sim A_\infty$) is the amount of sorbate taken up at steady state. The experimental data were fitted to the function in Eq. 7 using a computer program. The best fit was calculated through an optimization process, yielding the parameters D and β.

The β values for most of the systems studied were found to range between 0.05 and 0.06 s^{-1}, depending on the experimental pressure (i.e., the lower the pressure, the higher the β). The β values indicated that around 16 to 20 s ($1/\beta$) were required for the system to establish a finite surface concentration of the sorbate.

It should be also noted that the single-component diffusion Eq. 7 was used to calculate the diffusion coefficients during the counterdiffusion of *n*-hexane and 1-hexene and the codiffusion of *n*-heptane and *p*-xylene, in zeolite L under subcritical and supercritical conditions.

Results and Discussion

Heptane self-diffusion in zeolite L under sub–supercritical conditions

Figures 1 and 2 show the change of the integrated absorbance of the stretching frequencies of *n*-heptane (3,100–2,700 cm^{-1}) during successive sorption (Figure 1) and desorption (Figure 2) experiments performed at 350°C and variable pressures of 13.8, 27.6, 41.4 and 55.2 bar. The critical conditions of *n*-heptane are 267°C and 27.4 bar. The ex-

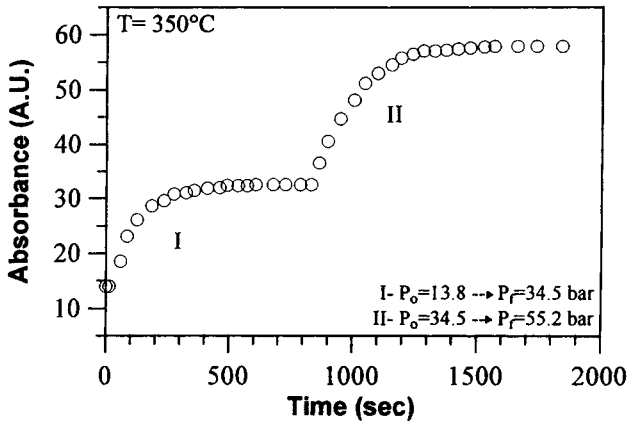

Figure 1. Integrated absorbance vs. time-on-stream during successive sorption of *n*-heptane from 13.8 bar to 55.2 bar, $\Delta P = 20.7$ bar.

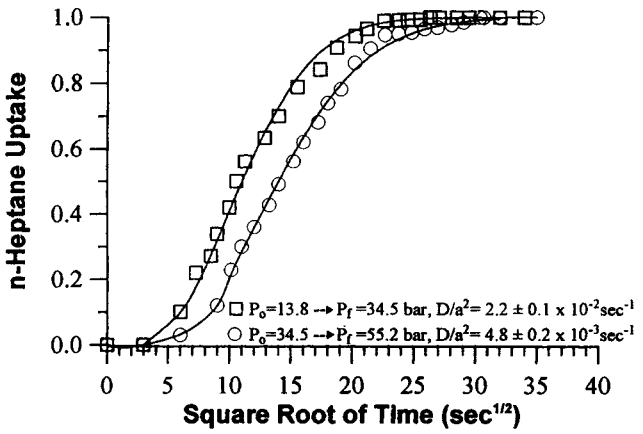

Figure 3. Self-diffusion of *n*-heptane in zeolite L at 350°C; symbols represent the experimental data, and solid lines represent the best fit.

periments were conducted by establishing equilibrium (constant heptane integrated absorbance) at an initial system pressure of P_0 followed by reducing (desorption) or increasing the pressure (sorption) at constant pressure intervals. It should be noted that at each final pressure (P_f) attained between intermediate sorption or desorption steps, equilibrium was established, as can be clearly seen from Figures 1 and 2.

The integrated absorbances at each time and pressure were evaluated by integrating the spectral region that corresponded to the stretching frequencies of *n*-heptane (3,100–2,700 cm^{-1}). In order to compensate for the small change in the refractive index due to a phase change in the system, the stretching modes of the hydrocarbons were ratioed to the zeolite framework vibrations (1,300–900 cm^{-1}) at each pressure. The obtained ratio was used as an internal standard to correct the changes in the penetration depth as a result of a phase change. The amount of sorbate taken at time t (absorbance, A_t) was ratioed to the steady-state value (A_∞) and the uptake curves shown in Figure 3 were obtained.

Figure 3 shows the uptake of *n*-heptane obtained during sorption measurements (increasing pressure) vs. square root of time. The symbols represent the experimental data, whereas the solid lines represent the best fit to Eq. 7 obtained by the computer program yielding D and β. The diffusion coefficients were computed by assuming an average crystallite radius of 0.3 μm. However, because of the uncertainty of the crystallite radius, the diffusion coefficients were expressed in terms of diffusion time constants (D/a^2). Furthermore, the particles showed a significant distribution in size (0.2 μm $< 2a <$ 1.2 μm).

From the best fits shown in Figure 3, a diffusion time constant of 2.2×10^{-2} s^{-1} was obtained at subcritical to supercritical transition region (P/P_c = 0.5 to 1.3), whereas 4.6 times lower diffusion time constant (4.8×10^{-3} s^{-1}) was obtained in the far supercritical regime (P/P_c = 1.3 to 2.0). The IR revealed that the density of *n*-heptane within the pores of zeolite L at the lowest pressure studied (13.6 atm, $P/P_c = 0.5$) was actually 10 times higher than the density of SCF at the same temperature evaluated by the equations of state. On the other hand, the density was almost 25–30 times higher than the corresponding SCF density (equations of state) at the highest pressure studied (55.2 bar, $P/P_c = 2.0$). The results also showed that the density of the fluid at supercritical conditions of 55.2 bar was actually 5.2 and 3.1 times higher than at subcritical conditions of 13.8 bar and supercritical conditions of 34.5 bar, respectively. Therefore, the reason for the decrease in the diffusion time constant from the subcritical–supercritical transition region to the far supercritical region could be attributed to the formation of a much denser phase under far supercritical conditions, which significantly reduced self-diffusion within the pores. This is consistent with the literature, which showed an exponential decay of the diffusion coefficient with respect to density (Lai and Tan, 1993). However, even at the lowest pressure of 13.8 bar, there is still a high-density fluid within the pores (10 times higher than the SCF density computed from the equations of state). Therefore, the calculated diffusion time constant of 0.022 s^{-1} should be much higher at lower densities, such as at 1 bar (gas phase).

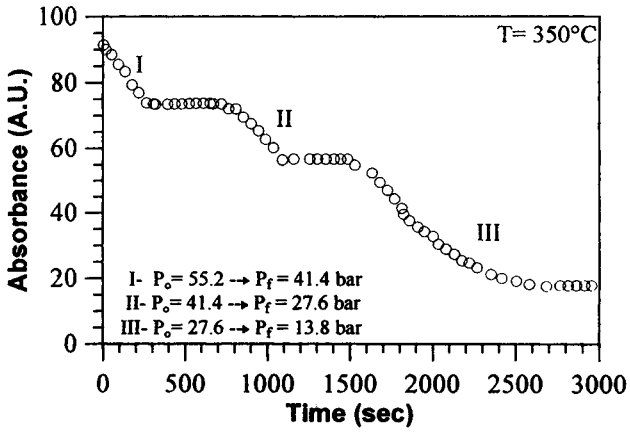

Figure 2. Integrated absorbance vs. time-on-stream during successive desorption of *n*-heptane from 55.2 bar to 13.8 bar, $\Delta P = 13.8$ bar.

Counterdiffusion of 1-hexene vs. n-hexane in zeolite L under subcritical and supercritical conditions

In most of the cracking reactions that were performed in the supercritical regime, we have consistently shown signifi-

cant increases in catalytic activities and paraffin-to-olefin ratios at supercritical conditions relative to subcritical conditions (Süer et al., 1996a,b; Dardas et al., 1996b). Therefore, our objective here was to understand the adsorption and diffusion characteristics of paraffins and especially olefins (i.e., route to coke formation) under subcritical and supercritical conditions.

The experiments were conducted by establishing equilibrium of *n*-hexane constant integrated absorbance) at a certain system pressure followed by the introduction of 1-hexene to the system by keeping the flow rate and total system pressure constant. Such a procedure provided a concentration gradient of 1-hexene within the micropores of zeolite L while all other variables were kept constant. This procedure was repeated for three different pressures in the subcritical and supercritical regimes. It should be noted that at each pressure, the system was reequilibrated with *n*-hexane before introducing 1-hexene. The critical temperature and pressure for *n*-hexane and 1-hexene are 235°C, 30.1 bar, and 231°C, 31.7 bar, respectively.

Figure 4 shows a set of infrared spectra acquired during successive states of uptake of 1-hexene by zeolite L at 300°C and 55.2 bar. The region presented corresponds to the stretching vibration modes of the feed hydrocarbon. As soon as 1-hexene was introduced to the system, the intensity of the 3,080 cm^{-1} band, which is characteristic of 1-hexene (C = C stretching mode), started to grow as a function of time, and the steady state was reached at 900 s.

The integrated absorbances for *n*-hexane and 1-hexene shown in Figure 5 at each time and pressure were calculated as follows: from a pure 1-hexene run at 300°C, a characteristic 1-hexene peak was located at 908 cm^{-1} in the fingerprint region. Using the area ratio of the stretching vibration region (3,100–2,700 cm^{-1}) to the 908 cm^{-1} peak for pure 1-hexene at 300°C, an internal standard was evaluated. This internal standard was used to evaluate the area of the 3,100–2,700 cm^{-1} region that corresponded to 1-hexene from the succes-

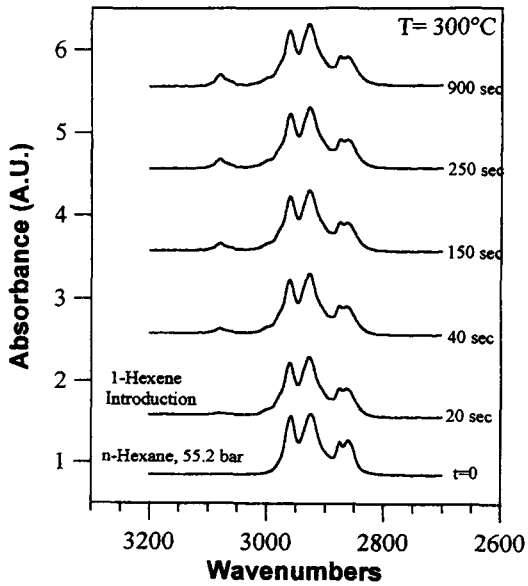

Figure 4. Set of IR spectra for successive states of sorption of 1-hexene at 300°C.

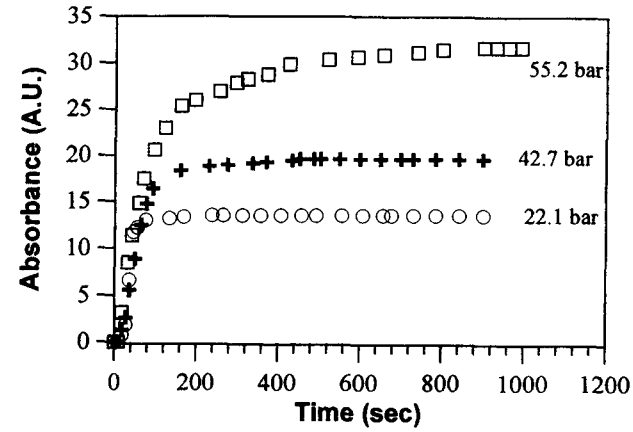

Figure 5. 1-Hexene absorbance vs. time-on-stream at 300°C and pressures of 22.1, 42.7 and 55.2 bar.

sive integration of the 908 cm^{-1} peak during the counter diffusion experiments. The evaluated area was successively subtracted from the total stretching area (3,100–2,700 cm^{-1}) and the *n*-hexane integrated absorbance between 3,100 and 2,700 cm^{-1} was calculated. The amount of sorbate taken at time *t* (absorbance, A_t) was ratioed to the steady-state value (A_α) at each pressure, and the uptake curves for 1-hexene shown in Figure 6 were obtained.

The best fits obtained from Figure 6 showed that a diffusion time constant of 4.0×10^{-3} s^{-1} was obtained for the counterdiffusion of 1-hexene vs. hexane in zeolite L at 22.1 bar and 300°C. The diffusion time constant decreased 1.7 and 5.6 times when the system pressure increased from 22.1 bar to 42.7 and 55.2 bar, respectively. The IR showed that the reduced density ($\rho_{(T,P)}/\rho_{(Liq,25°C)}$) of *n*-hexane before the introduction of 1-hexene (reequilibration points) at each pressure decreased from 0.80 to 0.45 and to 0.32 as the pressure was decreased from 55.2 to 42.7 and to 22.1 bar, respectively. These results showed that the increase in the density of *n*-hexane significantly reduced the diffusion of the counterdif-

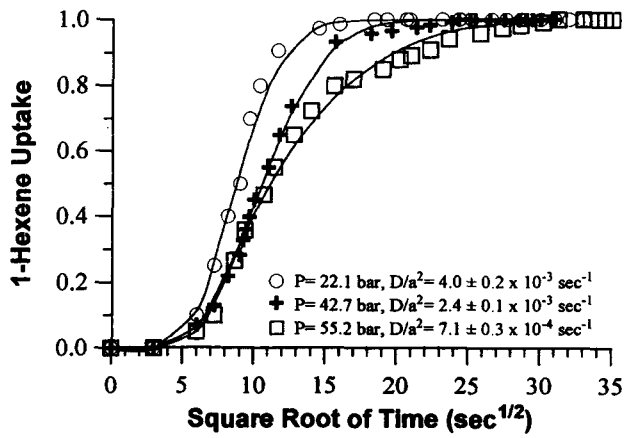

Figure 6. Counterdiffusion of 1-hexene vs. hexane in zeolite L at 300°C and pressures of 22.1, 42.7 and 55.2 bar.

Symbols represent the experimental data, and solid lines represent the best fit.

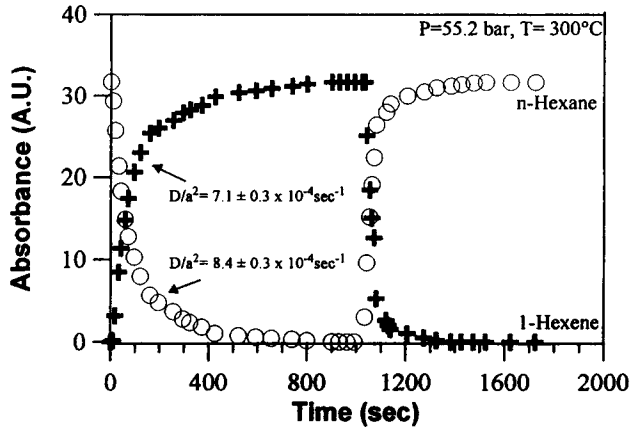

Figure 7. Absorbance vs. time-on-stream during the counterdiffusion of 1-hexene vs. *n*-hexane in zeolite L at 300°C and 55.2 bar.

fusing sorbate (1-hexene) as the pressure of the system was increased at constant intervals, or the diffusion of the counterdiffusing sorbate (1-hexene) increased as the system pressure was decreased.

The decrease of the partial pressure of *n*-hexane with 1-hexene introduction will result in the desorption of *n*-hexane from the acid sites. This will further be followed by the sorption of 1-hexene to these acid sites due to its increasing partial pressure. Figure 7 shows that when the olefin was introduced to the system under supercritical hexane conditions of 300°C and 55.2 bar, it displaced all the paraffin in 350–400 s. On the other hand, when the paraffin was introduced back into the system, it displaced all the olefin in 250–300 s. This was surprising since one would expect a relatively stronger adsorption of the olefin. The results also showed that uptake of the paraffin was faster than its desorption, and a faster paraffin uptake resulted in a faster desorption of the olefin. Thus, a faster establishment of the steady state was observed for both the paraffin and the olefin when the paraffin was introduced back into the system.

On the other hand, as shown in Figure 8, when the olefin was introduced to the system under subcritical *n*-hexane conditions of 22.1 bar, a much faster displacement of the paraffin with the olefin was observed (< 200 s). This clearly showed a faster diffusion of both components under subcritical conditions due to the lower densities of the sorbates.

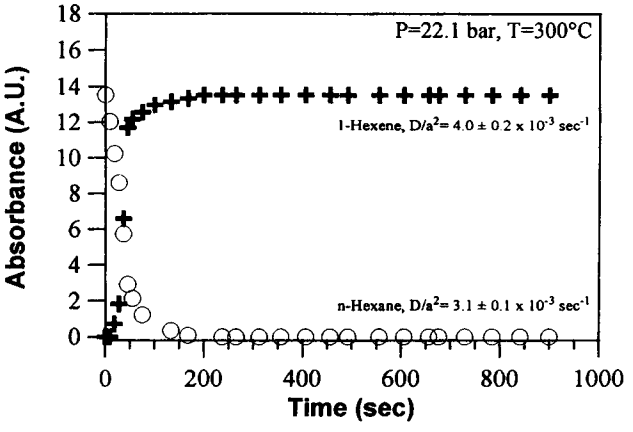

Figure 8. Absorbance vs. time-on-stream during the counter diffusion of 1-hexene vs. *n*-hexane in zeolite L at 300°C and 22.1 bar.

It should be noted that the extinction coefficient of a C–H moiety varies depending on the environment of C attached to H (i.e., alkane–C–H, alkene–C–H, aromatic–C–H). Thus, the integrated intensities of 1-hexene shown in Figures 5, 7, and 8 are corrected for the changes in the extinction coefficient of the C–H moiety due to the presence of a double bond. As a result, the absorbances for *n*-hexane and 1-hexene represent true concentrations.

The diffusion time constant of *n*-hexane ($D/a^2 = 8.4\times10^{-4}$ s^{-1}) was 1.2 times higher than 1-hexene ($D/a^2 = 7.1\times10^{-4}$ s^{-1}) under supercritical conditions of 300°C and 55.2 bar. However, under subcritical conditions of 300°C and 22.1 bar, the diffusion time constant of *n*-hexane ($D/a^2 = 3.1\times10^{-3}$ s^{-1}) was 1.3 times lower than 1-hexene ($D/a^2 = 4.0\times10^{-3}$ s^{-1}). Note that under subcritical conditions of 22.1 bar, the counterdiffusion of 1-hexene in zeolite L was 5.6 times faster when compared with supercritical conditions of 55.2 bar. Similarly, under subcritical conditions of 22.1 bar, the counterdiffusion of *n*-hexane in zeolite L was 3.7 times faster when compared with supercritical conditions of 55.2 bar.

The literature contains various studies that measured the intracrystalline diffusivities of gas and liquid-phase *n*-paraffins at room temperature (e.g., Wu et al., 1983; Karger and Pfeifer, 1987; Beschmann et al., 1990; Choudhary et al., 1992; Ruthven and Stapleton, 1993). Wu et al. (1983) reported a diffusion coefficient of 7.5×10^{-12} cm^2/s for *n*-hexane in silicalite at 30°C under subatmospheric conditions (gas phase). On the other hand, our study showed self-diffusion coefficients of 2×10^{-11} and 4.3×10^{-12} cm^2/s for *n*-heptane in zeolite L at 350°C in subcritical supercritical transition regimes ($P/P_c = 0.5$ to 1.3) and in the far supercritical regime ($P/P_c = 1.3$ to 2.0) respectively, when an average crystallite radius of 0.3 μm was considered. On the other hand, counterdiffusion studies showed counterdiffusion coefficients of 7.6×10^{-13} and 2.8×10^{-12} cm^2/s for *n*-hexane vs. 1-hexene in zeolite L at 300°C under supercritical conditions of 55.2 bar ($P/P_c = 1.83$), and subcritical conditions of 22.1 bar ($P/P_c = 0.74$), respectively. Although a legitimate comparison of our data with Wu et al.'s (1983) results is not possible due to the differences in sorbents and measurement conditions, the order of magnitudes of the diffusion coefficients obtained for *n*-heptane and *n*-hexane in zeolite L at high temperatures of 300–350°C under dense reaction media were similar to that obtained for gas-phase *n*-hexane under the low temperature of 30°C, obtained by Wu et al. (1983). However, since the diffusion coefficient increases exponentially with increasing temperature, the diffusion coefficient of 7.5×10^{-12} cm^2/s for *n*-hexane in HZSM-5 at 30°C, given by Wu et al. (1983), should be significantly higher at temperatures of 300–350°C. This can be better visualized from NMR relaxation studies conducted by Karger and Pfeifer (1987). They obtained a gas-phase diffusion coefficient of around 8×10^{-6} cm^2/s during *n*-heptane self-diffusion in about 4 μm NaX crystals at around 200°C. This value is almost five orders of magnitude higher than the diffusion coefficient obtained from our experiments for the self-diffusion of *n*-heptane in zeolite L at 350°C under dense reaction media. Such a significant differ-

ence predicted liquidlike behavior of the hydrocarbons within the pores of zeolite L, since the diffusion coefficients obtained under such high temperatures and high pressures are more liquidlike than gaslike. This observation is in complete agreement with the liquidlike densities observed within the micropores of microporous zeolites by the *in-situ* CIR-FTIR technique under high-temperature, high-pressure conditions (Süer, 1996a,b; Dardas et al., 1996b).

Codiffusion of an equimolar heptane/p-xylene mixture in zeolite L under subcritical and supercritical conditions

Codiffusion is particularly interesting in hydrocarbon separation processes where a mixture of a hydrocarbon feed is separated into pure components by the use of a suitable sorbent. Therefore, it is important to explore the adsorption and diffusion properties of hydrocarbon mixtures under subcritical and supercritical conditions.

The system analyzed was the codiffusion of heptane and *p*-xylene in zeolite L at 350°C and pressures ranging from 13.8 to 55.2 bar at constant pressure intervals. The experiments were conducted by feeding a 1:1 mixture of *n*-heptane and *p*-xylene to the system at a total system pressure of 55.2 bar. After the equilibrium was reached (constant integrated absorbance), the system pressure was reduced to 13.8 bar at constant intervals of 13.8 bar. From Kay's rule (Reid et al., 1987), the average critical conditions of the mixture were calculated at 305°C and 31.2 bar.

Figure 9 shows the change of the integrated absorbance of the stretching modes (3,100–2,700 cm^{-1}) of *n*-heptane and *p*-xylene during successive desorption of the hydrocarbon mixture at 350°C and variable pressures of 55.2, 41.4, 27.6 and 13.8 bar. The integrated absorbances at each time and pressure were evaluated as follows: from a pure *p*-xylene run at 350°C, a strong peak at 790 cm^{-1} was located (Figure 10, top graph, top spectra) in the fingerprint region (1,000–700 cm^{-1}), whereas *p*-xylene showed characteristic peaks in the stretching-vibration region between 3,100 and 2,700 cm^{-1} (Figure 10, bottom graph, top spectra). The ratio of the 790

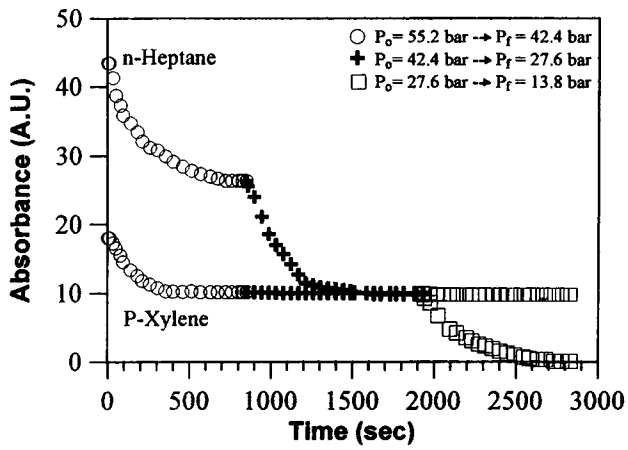

Figure 9. Absorbance vs. time-on-stream during successive desorption of an equal mixture of *n*-heptane and *p*-xylene from 55.2 to 13.8 bar, ΔP = 13.8 bar at 350°C.

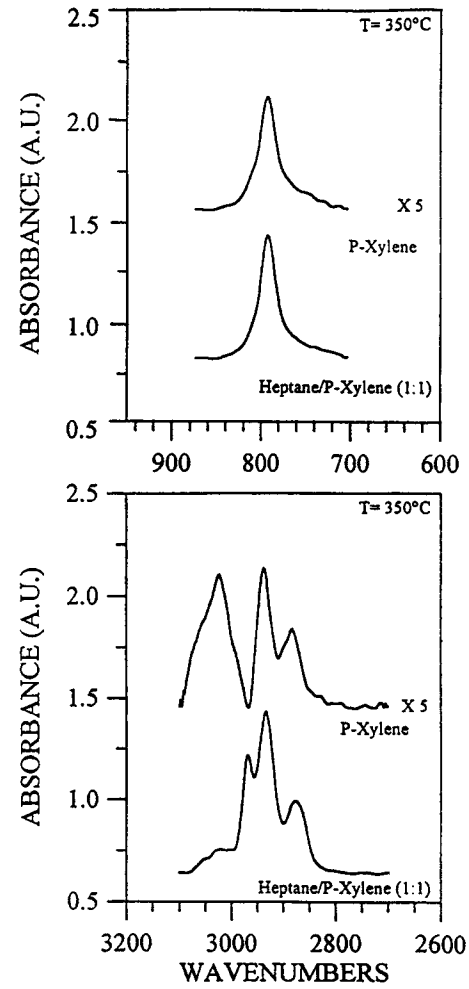

Figure 10. *First and second graph bottom spectra*, IR spectra during the codiffusion of heptane/*p*-xylene mixture (1:1) at 350°C, *P* = 55.2–41.4 bar; *First and second graph top spectra*, IR spectra of pure *p*-xylene at 350°C and 41.4 bar.

cm^{-1} peak area to the total area of peaks in the 3,100–2,700 cm^{-1} region for pure *p*-xylene was always at this temperature, independent of pressure changes. After evaluating this ratio, the total area of the stretching vibration region (3,100–2,700 cm^{-1}) during the codiffusion of the *n*-heptane and *p*-xylene (1:1) mixture was evaluated at each pressure as a function of time. This area corresponded to the total area of the C–H stretching modes of both *n*-heptane and *p*-xylene (Figure 10, bottom graph, bottom spectra). Also, the 790 cm^{-1} band (*p*-xylene) was evaluated at each pressure as a function of time during the co-diffusion of the *n*-heptane and *p*-xylene mixture (Figure 10, top graph, bottom spectra). Using the 790/3,100–2,700 cm^{-1} bands ratio, the area of *p*-xylene stretching modes (3,100–2,700 cm^{-1}) was calculated at each pressure and time, and successively subtracted from the total area (3,100–2,700 cm^{-1}) for the evaluation of the area of the *n*-heptane stretching modes. The amount of sorbate taken at time *t* (absorbance, A_t) was ratioed to the steady-state value (A_α) at each pressure, and the uptake curves for *n*-heptane during the codiffusion of an equal mixture of *n*-heptane and

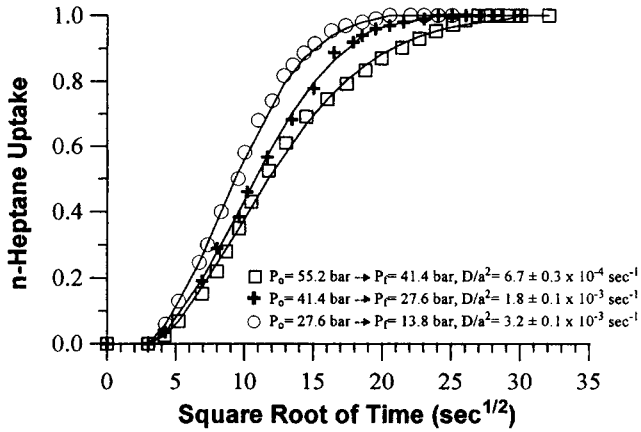

Figure 11. *n*-Heptane uptake during the codiffusion of an equal mixture of *n*-heptane and *p*-xylene at $T = 350°C$ and variable pressures of 55.2, 41.4, 27.6, and 13.8 bar.

Symbols represent the experimental data, and solid lines represent the best fit.

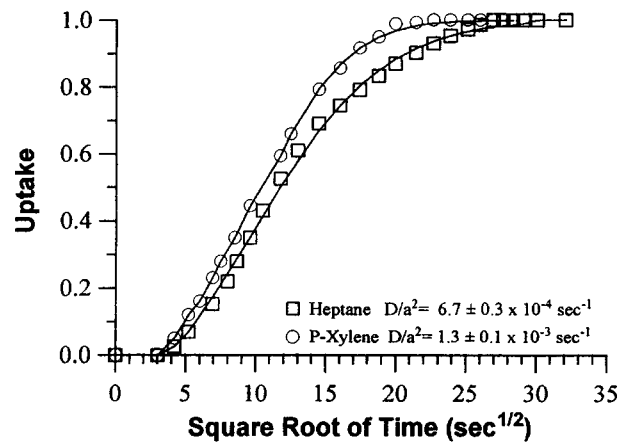

Figure 12. Codiffusion of an equal mixture of *n*-heptane and *p*-xylene under supercritical conditions of $T = 350°C$ and pressures from 55.2 to 41.4 bar.

Symbols represent the experimental data and solid lines represent the best fit.

p-xylene under subcritical and supercritical conditions are shown in Figure 11.

It should be also noted that the integrated intensities of *p*-xylene shown in Figure 9 are corrected for the changes in the extinction coefficient of the C–H moiety due to the presence of the aromatic ring. Thus, the absorbances for *n*-heptane and *p*-xylene represent true concentrations. This indicated that even when a 1:1 heptane/*p*-xylene mixture was fed to the system initially, the corrected integrated intensities shown in Figure 9 revealed a higher concentration of *n*-heptane within the pores of zeolite L under supercritical conditions due to the steric constraints for the bulky *p*-xylene molecule.

The best fits obtained from Figure 11 showed a diffusion time constant of 6.7×10^{-4} s^{-1} for *n*-heptane during the codiffusion of an equal mixture of *p*-xylene and *n*-heptane well in the supercritical regime ($P = 55.2$ to 41.4 bar), whereas a 2.7 and 4.6 times higher diffusion time constants were obtained in the subcritical–supercritical transition region ($P =$ 41.4 to 27.6 bar) and well in the subcritical regime ($P = 27.6$ to 13.8 bar), respectively. The diffusion time constants obtained for *n*-heptane during the codiffusion experiments were almost one order of magnitude lower than the values obtained for *n*-heptane during the self-diffusion experiments, as expected. However, the most interesting aspect of the data was the instantaneous adsorption of *p*-xylene under near-critical (41.4 to 27.6 bar) and subcritical conditions (27.6 to 13.8 bar), shown in Figure 9. The infrared analysis showed almost a constant integrated absorbance of *p*-xylene under these conditions, indicating no desorption of *p*-xylene with reducing pressure. However, in the far supercritical regime (55.2 to 41.4 bar), the strong adsorption of *p*-xylene was not observed. The infrared results showed that the observed integrated absorbance for *p*-xylene was about 50% of its initial absorbance after the pressure was reduced from 55.2 to 41.4 bar (Figure 9). The diffusion time constants evaluated under these conditions showed that the diffusion of *p*-xylene (1.3×10^{-3} s^{-1}) was 1.9 times faster than *n*-heptane (5.3×10^{-4} s^{-1}) (Figure 12).

The unusual transport behavior of *p*-xylene relative to *n*-heptane observed under far supercritical conditions (faster diffusion, Figure 12) is believed to also be a result of the abrupt increase of the density of the hydrocarbons (i.e., heptane) within the pores under supercritical conditions, which resulted in a competitive adsorption by the continuous extraction of the adsorbed species (i.e., *p*-xylene) by the dense, SCF (i.e., *n*-heptane). This might be crucial for hydrocarbon conversion processes rather than the separation processes, where a high rate of diffusion of the bulky product relative to a linear product could be obtained under a dense, supercritical reaction medium. On the other hand, under subcritical conditions, where the hydrocarbon density was much lower, a strong adsorption of *p*-xylene was observed.

On the other hand, literature studies that measured the intracrystalline diffusion coefficients for *p*-xylene in HZSM-5 and silicalite at 25°C under subatmospheric conditions are listed in Table 1. From the reported crystallite radii, the diffusion time constants for *p*-xylene in HZSM-5 and silicalite are evaluated and also presented in Table 1.

Table 1 showed that the gas-phase diffusion time constants obtained for *p*-xylene in HZSM-5 ranged between 10^{-1} to 10^{-3} s^{-1}. Again, even a direct comparison of our data with those in studies in the literature is not possible due to the differences in sorbents, and measurement conditions, the or-

Table 1. Diffusion of *P*-Xylene in HZSM-5 and Silicalite at 20–25°C

Sorbent	$r(\mu m)$	$D(cm^2/s)$	$D/r^2(s^{-1})$	Reference
HZSM-5	1.5	3.0×10^{-11}	1.3×10^{-3}	Beschmann et al. (1987)
HZSM-5	1.8	6.0×10^{-11}	1.9×10^{-3}	Prinz and Riekert (1986)
HZSM-5	0.3	3.0×10^{-11}	3.0×10^{-2}	Nayak and Riekert (1985)
HZSM-5*	3 **	8.5×10^{-11}	9.4×10^{-3}	Niessen and Karge (1993)
Silicalite	1	1.0×10^{-11}	1.0×10^{-3}	Wu et al. (1983)
Silicalite	27.5	4.0×10^{-10}	5.3×10^{-1}	Ruthven et al. (1991)

*The diffusion coefficient has been measured at 125°C.
**The crystallite radius was estimated from the reported dimensions ($8 \times 5 \times 3 = 4/3\pi R^3$).

Table 2. Summary of Diffusion Time Constants

Method	Hydrocarbon	T(°C)	P_0(bar)	P_f(bar)	ΔP	$D/a^2 \times 10^3$(s^{-1})
Self-diffusion	*n*-Heptane	350	13.8	34.5	20.7	22.0
Self-diffusion	*n*-Heptane	350	34.5	55.2	20.7	4.80
Codiffusion	*n*-Heptane	350	55.2	41.4	13.8	0.67
Equilmolar *n*-	*p*-Xylene	350	55.2	41.4	13.8	1.30
heptane-*p*-xylene	*n*-Heptane	350	41.4	27.6	13.8	1.80
mixture	*n*-Heptane	350	27.6	13.8	13.8	3.20
Counter diffusion	1-Hexene	300	22.1			4.00
1-Hexene vs.	*n*-Hexane	300	22.1			3.10
n-hexane	1-Hexene	300	42.7			2.40
	1-Hexene	300	55.2			0.71
	n-Hexane	300	55.2			0.84

der of magnitude of the diffusion time constant obtained for *p*-xylene (1.3×10^{-3} s^{-1}) in zeolite L at 350°C and 55.2 bar, were similar to that obtained for gas-phase *p*-xylene under the low temperature of 25°C (Table 1). However, when the effect of temperature on the diffusion coefficient is considered again, the diffusion time constant reported for gas-phase *p*-xylene at 25°C in Table 1 should be significantly higher at temperatures of 300–350°C. For instance, Ruthven et al. (1991) reported a gas-phase diffusion coefficient of 3×10^{-8} cm^2/s for *p*-xylene in silicalite at 200°C. Using the reported crystallite radius (Table 1), a diffusion time constant around 40 s^{-1} was obtained. This number was almost two orders of magnitude higher than the number they measured for vapor-phase *p*-xylene at 25°C under subatmospheric conditions (Table 1) and almost five orders of magnitude higher than the value obtained in this study for *p*-xylene under supercritical conditions ($P = 55.2$ to 41.4 bar). Therefore, once again, the diffusion coefficients obtained for *p*-xylene in zeolite L under dense reaction media clearly showed a liquidlike behavior of the aromatic hydrocarbon (*p*-xylene) within the pores of the zeolite.

Conclusions

The CIR-FTIR technique was successfully applied to determine the transport properties of supercritical hydrocarbons within porous catalysts. To our knowledge, this was the first time that the intracrystalline diffusion coefficients of hydrocarbons could be measured under supercritical conditions. Furthermore, these results are important to industrial processes employing porous catalysts at high temperatures, since the CIR-FTIR technique affords a direct measurement of the transport properties of reactants and products under dynamic conditions, typical of industrial applications.

The results (summarized in Table 2) obtained during the self-diffusion of *n*-heptane, counter-diffusion of 1-hexene vs. *n*-hexane, and codiffusion of an *n*-heptane/*p*-xylene mixture in zeolite L under subcritical and supercritical conditions of the hydrocarbons studied showed that the diffusion within the pore was significantly reduced under supercritical conditions (i.e., liquidlike behavior) as the hydrocarbon density within the pore increased.

Acknowledgments

The authors acknowledge the Air Force Office of Scientific Research for financial support of this study under Grant Contract AFOSR G:F49620-93-1-0204.

Literature Cited

Baptist-Nguyen, S., and B. Subramaniam, "Coking and Activity of Porous Catalysts in Supercritical Reaction Media," *AIChE J.*, **38,** 1027 (1992).

Barrer, R. M., and H. Villiger, "Crystal Structure of Synthetic Zeolite L," *Kristallography*, **128,** 352 (1969).

Barrer, R. M., *Zeolites and Clay Minerals as Sorbents and Molecular Sieves*, Academic Press, London (1978).

Beschmann, K., G. T. Kokotailo, and L. Riekert, "Kinetics of Sorption of Aromatics in Zeolite ZSM-5," *Chem. Eng. Process*, **22,** 223 (1987).

Beschmann, K., S. Fuchs, and L. Riekert, "Kinetics of Sorption of Benzene and *n*-Paraffins in Large Crystals of MFI Zeolites," *Zeolites*, **10,** 798 (1990).

Crank, J., *Mathematics of Diffusion*, Oxford Univ. Press, London (1956).

Choudhary, V. R., V. S. Nayak, and A. S. Mamman, "Diffusion of Straight and Branched Chain Liquid Compounds in H-ZSM-5 Zeolite," *Ind. Eng. Chem. Res.*, **31,** 624 (1992).

Dahmen, N., A. Kordikowski, and M. Schneider, "Determination of Binary Diffusion Coefficients of Organic Compounds in Supercritical Carbon Dioxide by Supercritical Fluid Chromatography," *J. Chromatog.*, **505,** 169 (1990).

Dardas, Z., M. G. Süer, Y. H. Ma, and W. R. Moser, "High Temperature, High Pressure *in situ* Reaction Monitoring of Heterogeneous Catalytic Processes under Supercritical Conditions by CIR-FTIR," *J. Catal.*, **159,** 204 (1996a).

Dardas, Z., M. G. Süer, Y. H. Ma, W. R. Moser, "A Kinetic Study of *n*-Heptane Catalytic Cracking over a Commercial Y-Type Zeolite under Supercritical and Subcritical Conditions," *J. Catal.*, **162,** 327 (1996b).

Derouane, E.G., and D. J. Vanderveken, "Structural Recognition and Preorganization in Zeolite Catalysis: Direct Aromatization of *n*-Hexane on Zeolite L Based Catalysts," *Appl. Catal.*, **45,** L15 (1988).

Eic, M., D. M. Ruthven, "A New Experimental Technique for Measurement of Intracrystalline Diffusivity," *Zeolites*, **8,** 40 (1988).

Ginosar, D. M., and B. Subramaniam, "Olefinic Oligomer and Cosolvent Effects on the Coking and Activity of a Reforming Catalyst in Supercritical Reaction Mixtures," *J. Catal.*, **152,** 31 (1995).

Jacob Sun, C. K., and S. H. Chen, "Tracer Diffusion of Aromatic Hydrocarbons on *n*-Hexane up to the Supercritical Region," *Chem. Eng. Sci.*, **40,** 2217 (1985).

Karge, H. G., and W. Niessen, "A New Method for the Study of Diffusion and Counterdiffusion in Zeolites," *Catal. Today*, **8,** 451 (1991).

Karger, J., and J. Caro, "Interpretation and Correlation of Zeolitic Diffusivities Obtained from NMR and from Sorption Experiments," *J. Chem. Soc. Faraday Trans. I*, **73,** 1363 (1977).

Karger, J., H. Pfeifer, M. Rauscher, and A. Walter, "Self Diffusion of *n*-Paraffins in NaX Zeolite," *J. Chem. Soc. Faraday Trans. I*, **76,** 717 (1980).

Karger, J., "A Study of Fast Tracer Desorption in Molecular Sieve Catalysts," *AIChE J.*, **28,** 417 (1982).

Karger, J., and H. Pfeifer, "N.M.R. Self-Diffusion Studies in Zeolite Science and Technology," *Zeolites*, **7,** 90 (1987).

Kiran, E., and J. F. Brenenecke, "Current State of Supercritical Fluid Science and Technology," *Supercritical Fluid Engineering Science:*

Fundamentals and Applications, E. Kiran and J. F. Brennecke, eds., ACS Symp. Ser., Vol. 514, American Chemical Society Books, Washington, DC, p. 1 (1993).
Lai, C. C., and C. S. Tan, "Measurement of Effective Diffusivities of Toluene in Activated Carbon in the Presence of Supercritical Carbon Dioxide," *Ind. Eng. Chem. Res.*, **32,** 1717 (1993).
Lang, X., A. Akgerman, and D. B. Bukur, "Steady State Fischer-Tropsch Synthesis in Supercritical Propane," *Ind. Eng. Chem. Res.*, **34,** 72 (1995).
Lin, Y. S., and Y. H. Ma, "A Comparative Study of Adsorption and Diffusion of Vapor Alcohols from Aqueous Solutions in Silicalite," *Zeolites: Facts, Figures Future*, P. A. Jacobs, and van Santen, eds., Elsevier, Amsterdam, p. 877 (1989a).
Lin, Y. S., and Y. H. Ma, "A Comparative Chromatographic Study of Liquid Adsorption and Diffusion in Microporous and Macroporous Adsorbents," *Ind. Eng. Chem. Res.*, **28,** 662 (1989b).
Lin, Y. S., and Y. H. Ma, "Analysis of Liquid Chromatography with Nonuniform Crystallite Particles," *AIChE J.*, **36,** 1569 (1990).
Ma, Y. H., Y. S. Lin, and H. L. Fleming, "Adsorption and Diffusion of Polar and Nonpolar Liquids in Aluminas by HPLC," *AIChE Symp. Ser.*, **84,** 1 (1988).
Manos, G., and H. Hoffman, "Coke Removal from a Zeolite Catalyst by Supercritical Fluids," *Chem. Eng. Technol.*, **14,** 73 (1991).
Moser, W. R., J. E. Cnossen, A. W. Wang, and S. A. Krouse, "Cylindrical Internal Reflectance: A New Method for High-Pressure *in situ* Reaction Studies," *J. Catal.*, **95,** 21 (1985).
Moser, W. R., "Reaction Monitoring by High Pressure Cylindrical Internal Reflectance and Optical Fiber Coupled Reactors," *Homogeneous Transition Metal Catalyzed Reactions*, W. R. Moser and D. W. Slocum, eds., Adv. Chem. Ser., Vol. 230, American Chemical Society Books, Washington, DC, p. 1 (1992).
Nayak, V. S., and L. Riekert, "Factors Influencing Sorption, and Diffusion in Pentasil Zeolites," *Acta Phys. Chem.*, **31,** 157 (1985).
Niessen, W., and H. G. Karge, "Diffusion of *p*-Xylene in Single and Binary Systems in Zeolites Investigated by FTIR Spectroscopy," *Microporous Mater.*, **1,** 1 (1993).
Prinz, D., and L. Riekert, "Observation of Rates of Sorption and Diffusion in Zeolite Crystals at Constant Temperature and Pressure," *Ber. Bunsenges. Phys. Chem.*, **90,** 413 (1986).
Reid, R. C., J. M. Prausnitz, and B. E. Poling, *The Properties of Gases & Liquids*, 4th ed., McGraw-Hill, New York, (1987).
Resing, H. A., "Nuclear Magnetic Resonance Relaxation of Molecules Adsorbed on Surfaces," *Adv. Mol. Relax. Processes*, **1,** 109 (1967/1968).
Riekert, L., "Sorption, Diffusion and Catalytic Reaction in Zeolites," *Adv. Catal. Relat. Subst.*, **21,** 281 (1970).
Riekert, L., "Rates of Sorption and Diffusion of Hydrocarbons in Zeolites," *AIChE J.*, **17,** 446 (1971).
Ruthven, D. M., *Principles of Adsorption and Adsorption Processes*, Wiley, New York (1984).
Ruthven, D. M., E. Mladen, and E. Richard, "Diffusion of C_8 Aromatic Hydrocarbons in Silicalite," *Zeolites*, **11,** 647 (1991).
Ruthven, D. M., and P. Stapleton, "Measurement of Liquid Phase Counter-Diffusion in Zeolite Crystals by the ZLC Method," *Chem. Eng. Sci.*, **48,** 89 (1993).
Saim, S., and B. Subramaniam, "Isomerization of 1-Hexene on Pt/γ-Al_2O_3 Catalyst at Subcritical and Supercritical Conditions: Pressure and Temperature Effects on Catalyst Activity," *J. Supercrit. Fluids*, **3,** 214 (1990).
Saim, S., and B. Subramaniam, "Isomerization of 1-Hexene over Pt/γ-Al_2O_3 Catalyst: Reaction Mixture Density and Temperature Effects on Catalyst Effectiveness Factor, Coke Laydown, and Catalyst Micromeritics," *J. Catal.*, **131,** 445 (1991).
Savage, P. E., S. Gopalan, T. I. Mizan, C. J. Martino, and E. E. Brock,"Reactions at Supercritical Conditions: Applications and Fundamentals," *AIChE J.*, **41,** 1723 (1995).
Squires, T. G., C. G. Venier, and T. Aida, "Supercritical Fluid Solvents in Organic Chemistry," *Fluid Phase Equilib.*, **10,** 261 (1983).
Subramaniam, B., and B. J. McCoy, "Catalyst Activity Maintenance or Decay: A Model for Formation and Desorption of Coke, *Ind. Eng. Chem. Res.*, **33,** 504 (1994).
Süer, M. G., Z. Dardas, Y. H. Ma, and W. R. Moser, "An *in-situ* CIR-FTIR Study *n*-Heptane Catalytic Cracking over a Commercial Y-Type Zeolite under Supercritical and Subcritical Conditions," *J. Catal.*, **162,** 320 (1996a).
Süer, M. G., Z. Dardas, Y. H. Ma, and W. R. Moser, "Performance of Different Zeolites during *n*-Heptane Catalytic Cracking under Supercritical Conditions," *J. Catal.* (1996b).
Tiltscher, H., H. Wolf, and J. Schelchhorn, "A Mild and Effective Method for the Reactivation or Maintenance of Activity of Heterogeneous Catalyst," *Angew. Chem. Int. Ed.*, **20,** 892 (1981).
Tiltscher, H., H. Wolf and J. Schelchhorn, "Utilization of Supercritical Fluid Solvents Effects in Heterogeneous Catalysis," *Ber. Bunsenges, Phys. Chem.*, **88,** 897 (1984).
Tiltscher, H., and H. Hoffman, "Trends in High Pressure Chemical Reaction Engineering," *Chem. Eng. Sci.*, **45,** 5 (1987).
Wu, P., A. Debebe, and Y. H. Ma, "Adsorption and Diffusion of C_6 and C_8 Hydrocarbons in Silicalite," *Zeolites*, **3,** 118 (1983).
Yokota, K., and K. Fujimoto, "Supercritical Phase Fischer-Tropsch Synthesis Reaction: 2. The Effective Diffusion of Reactant and Products in the Supercritical Phase Reaction," *Ind. Eng. Chem. Res.*, **30,** 95 (1991).

Manuscript received Sept. 12, 1996, and revision received Feb. 18, 1997.